Supporting Information

Influence of the regioregularity on the chiral supramolecular organization of poly(3-alkylsulfanylthiophene)s.

Helmuth Peeters, Pauline Couturon, Steven Vandeleene, David Moerman, Philippe Leclère, Roberto Lazzaroni, Inge De Cat, Steven De Feyter and Guy Koeckelberghs

Table of contents

S1. STM

S1.1 Fourier transformation

A

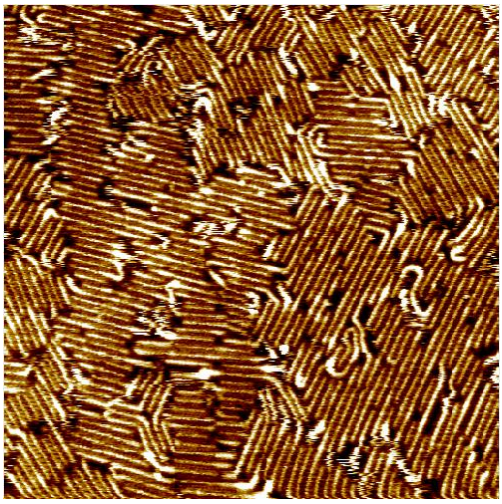

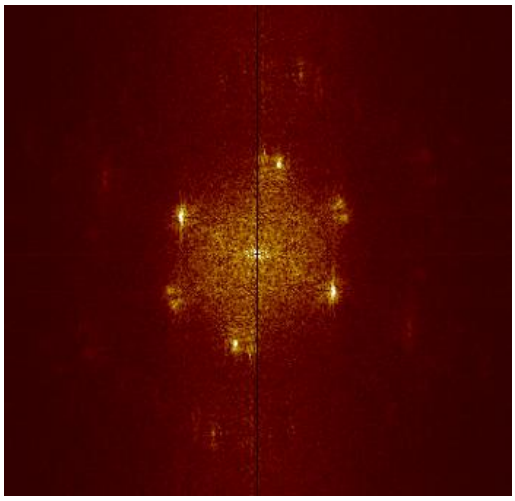

Size: 97.2 × 97.2 nm^2
I_{set}=127pA, V_{set}=-860mV

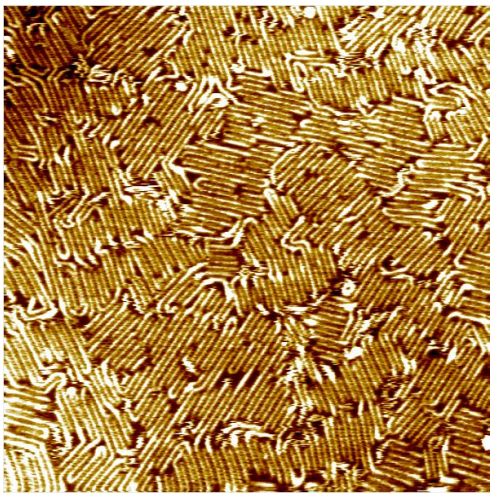

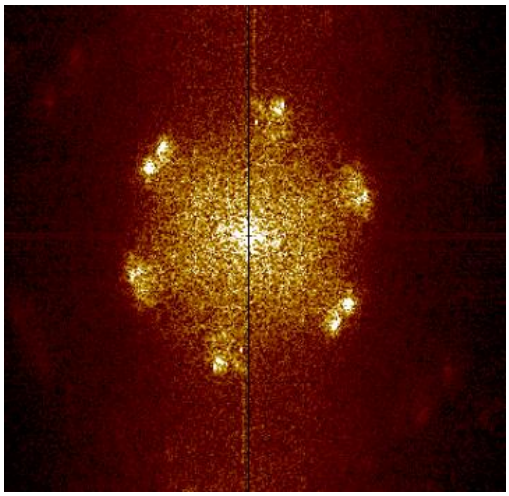

Size: 119 × 119 nm^2
I_{set}=127pA, V_{set}=-860mV

B

Fourier Analysis

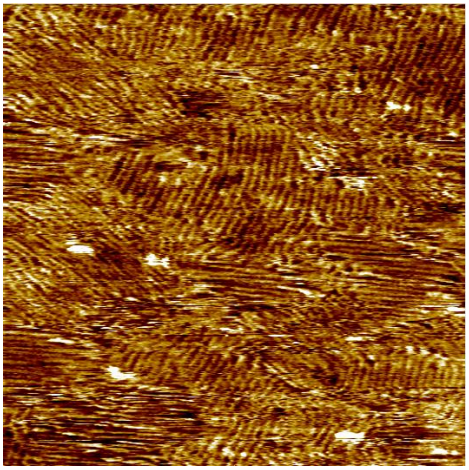

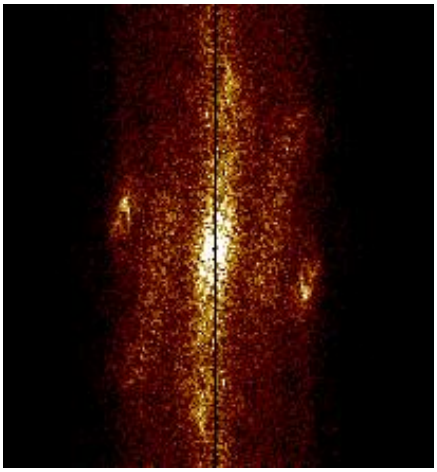

Size: 96.4 × 96.4 nm^2
I_{set}=189pA, V_{set}=-680mV

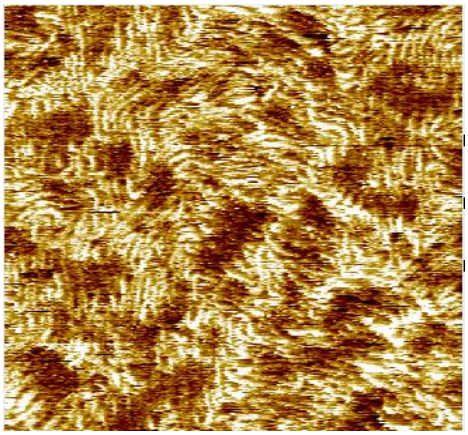

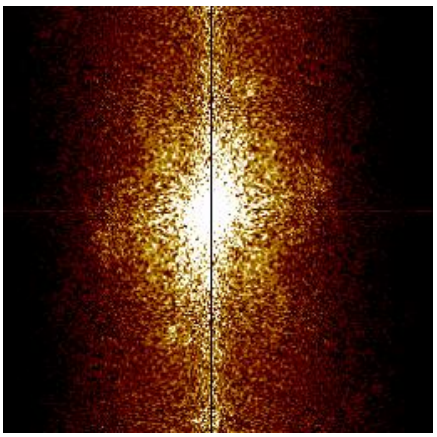

Size: 104 × 104 nm^2
I_{set}=127pA, V_{set}=-860mV

Figure S 1. STM images and the Fourier transformation of the regioregular P3AST (A) and regio-irregular P3AST (B) at the 1,2,4-TCB/graphite interface. The polymers used are the same as described in Macromolecules, 2008, 41, 5123-5131.

S1.2 Histograms

A

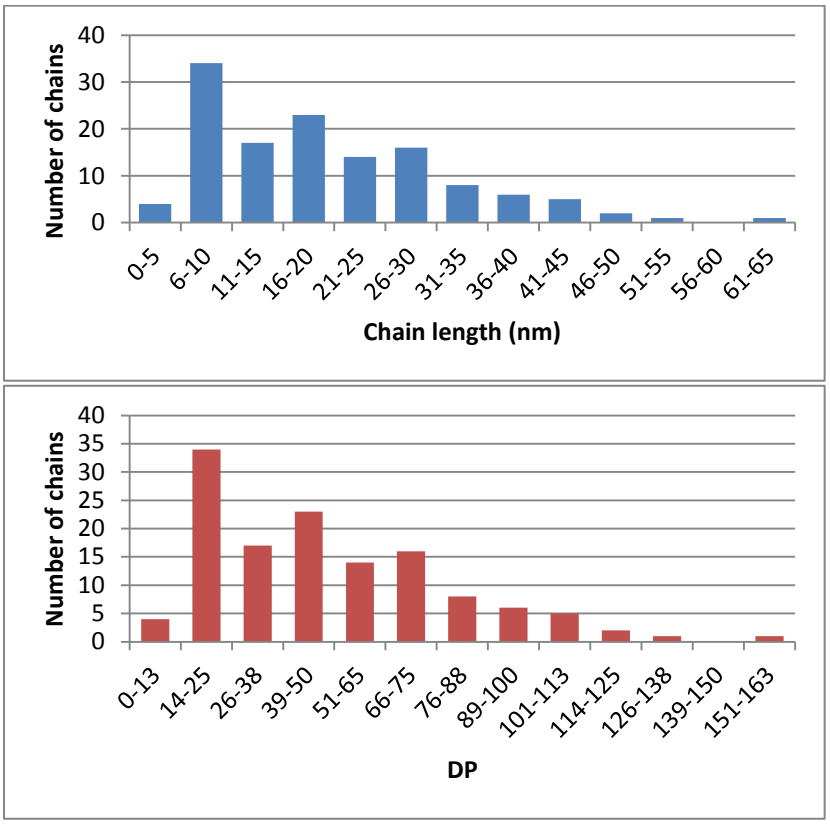

B

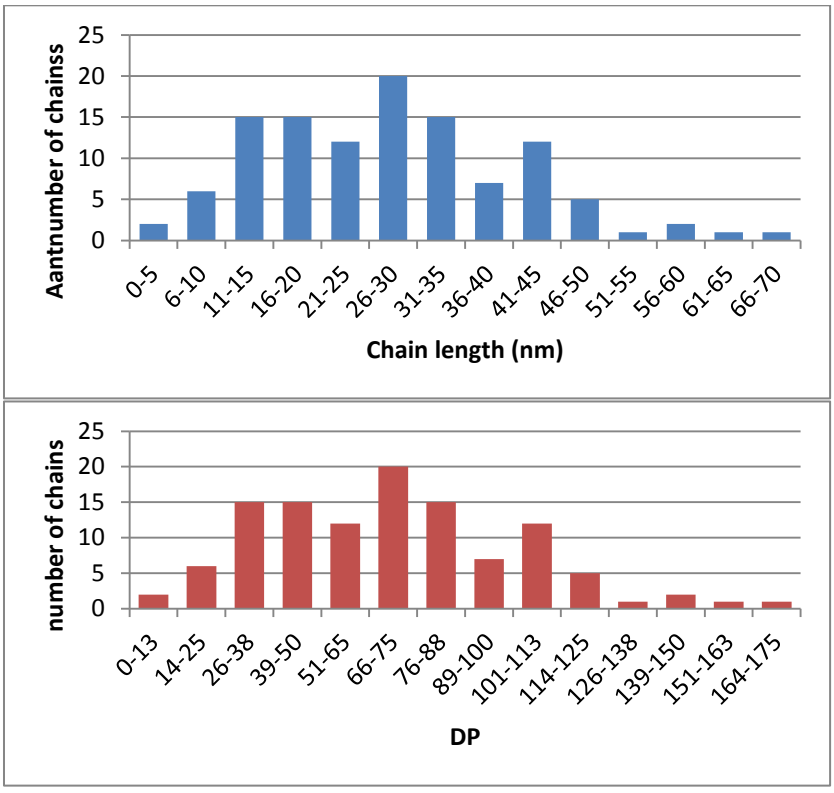

Figure S 2. Histograms showing the distribution of the lengths and DP of self-assembled of the regioregular P3AST (A) and the regio-irregular P3AST (B) chains at the 1,2,4-TCB/graphite interface.

S2. ^{1}H NMR spectra

S2.1 ^{1}H NMR spectrum of quench 2a' and (2a + 2b) with D_2O

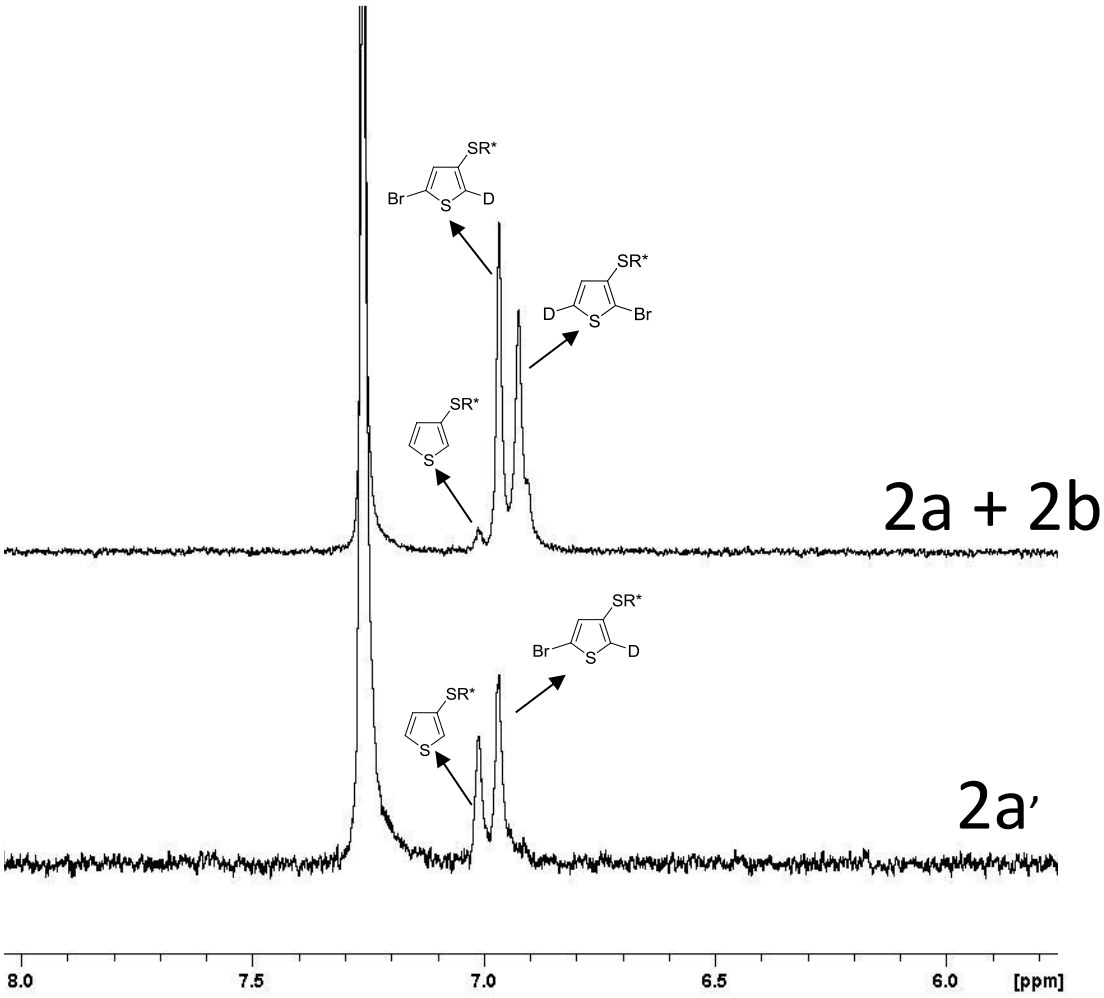

Figure S 3. ^{1}H NMR ($CDCl_3$) of the aromatic region of the quench of **2a'** and (**2a** + **2b**) with D_2O.

S2.2 ^{1}H NMR spectrum of P1

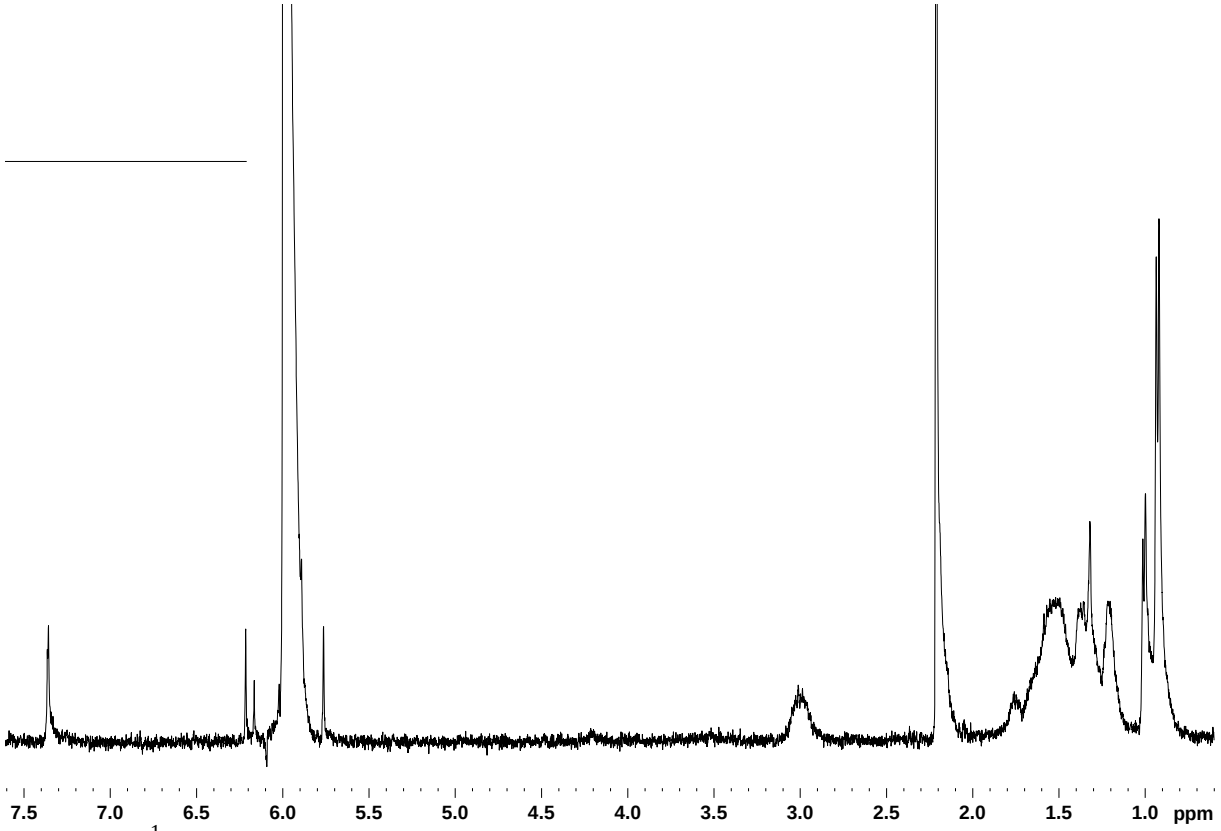

Figure S 4. ^{1}H NMR ($CS_2/C_2D_2CL_4$) of **P1**.

S2.3 ^{1}H NMR spectrum of P2

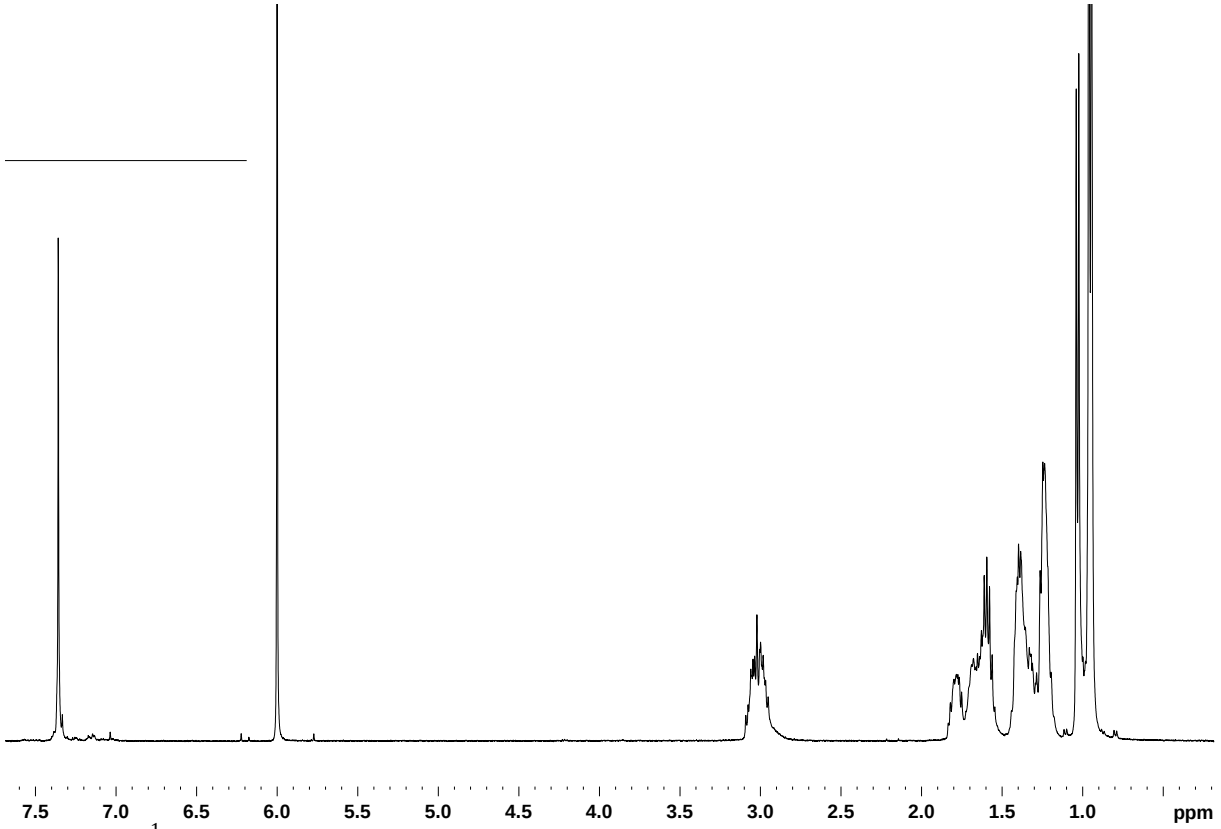

Figure S 5. ^{1}H NMR ($CS_2/C_2D_2CL_4$) of **P2**.

S2.4 ^{1}H NMR spectrum of P3

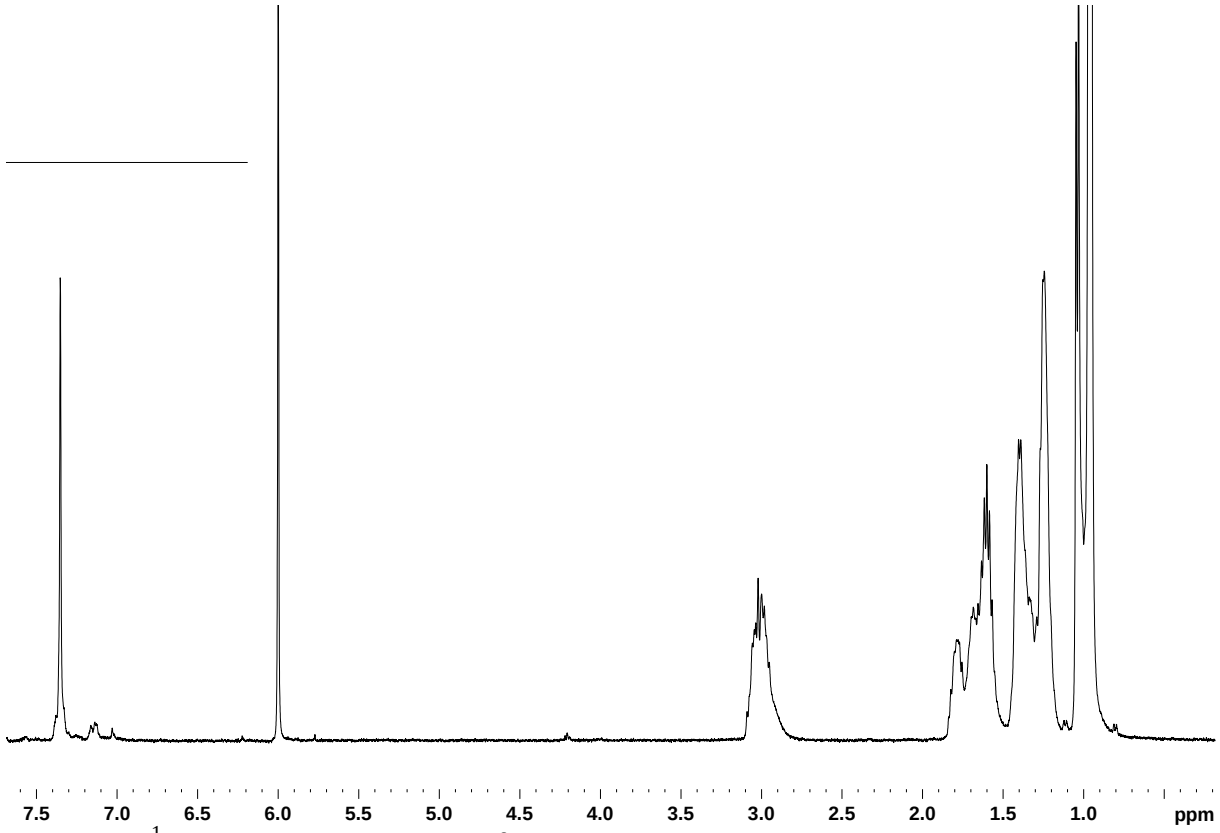

Figure S 6. ^{1}H NMR ($CS_2/C_2D_2CL_4$) of **P3**.

S2.5 ^{1}H NMR spectrum of P4

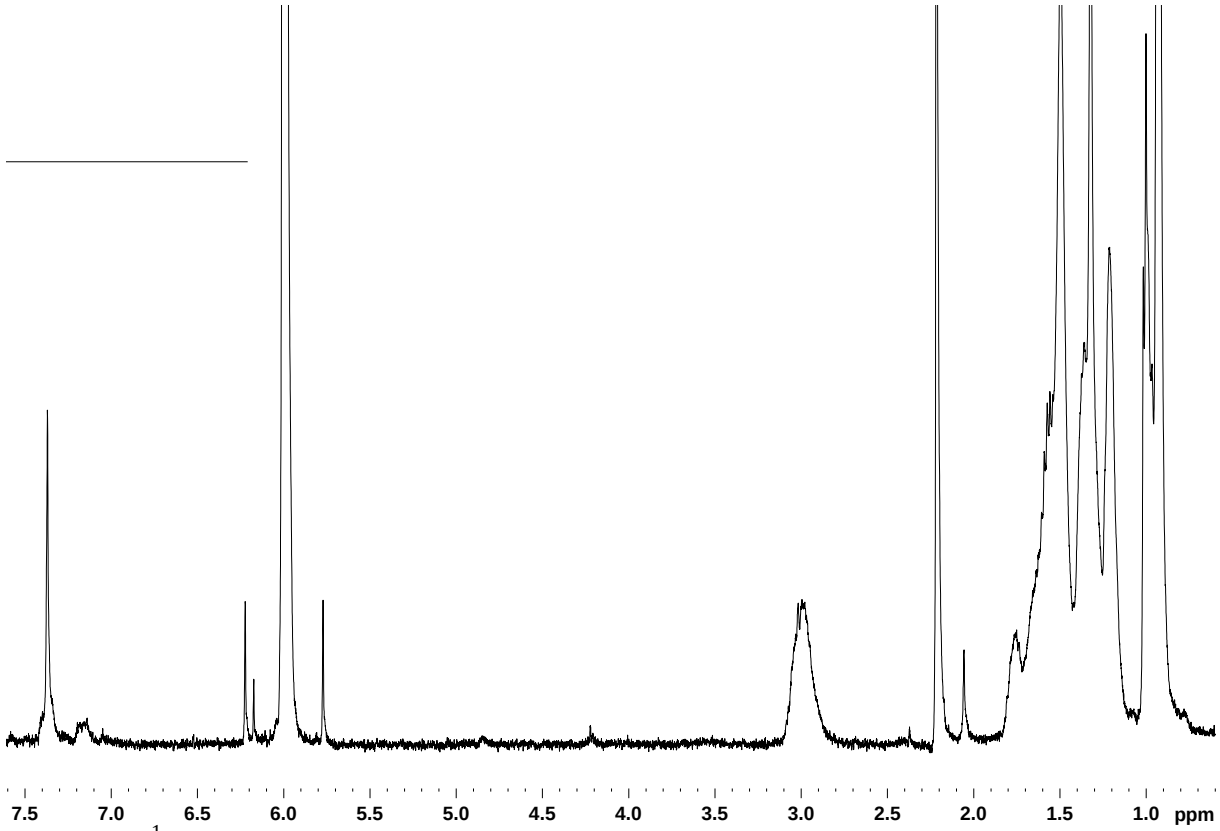

Figure S 7. ^{1}H NMR ($CS_2/C_2D_2CL_4$) of **P4**.

S2.6 ^{1}H NMR spectrum of P5

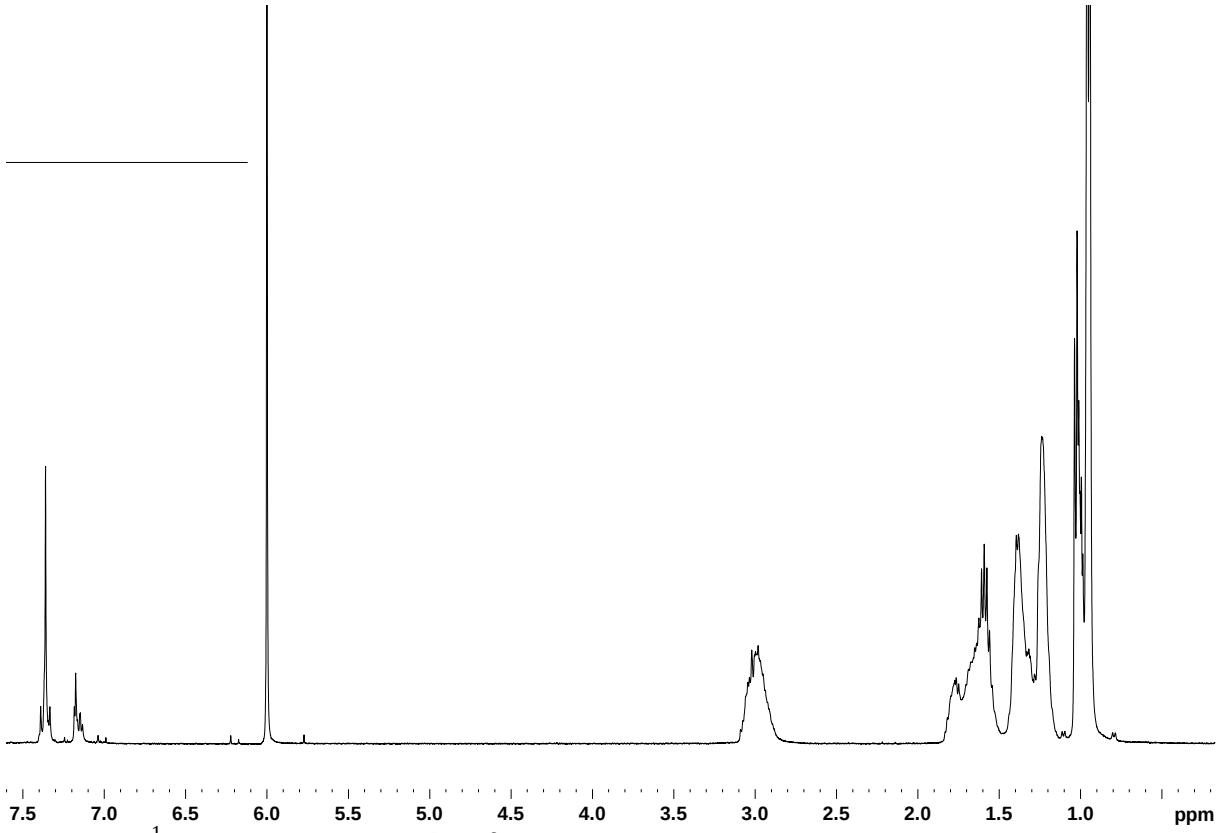

Figure S 8. ^{1}H NMR ($CS_2/C_2D_2Cl_4$) of **P5**.

S3. UV-vis spectra

S3.1 P1 and P2 in $CHCl_3/CS_2$

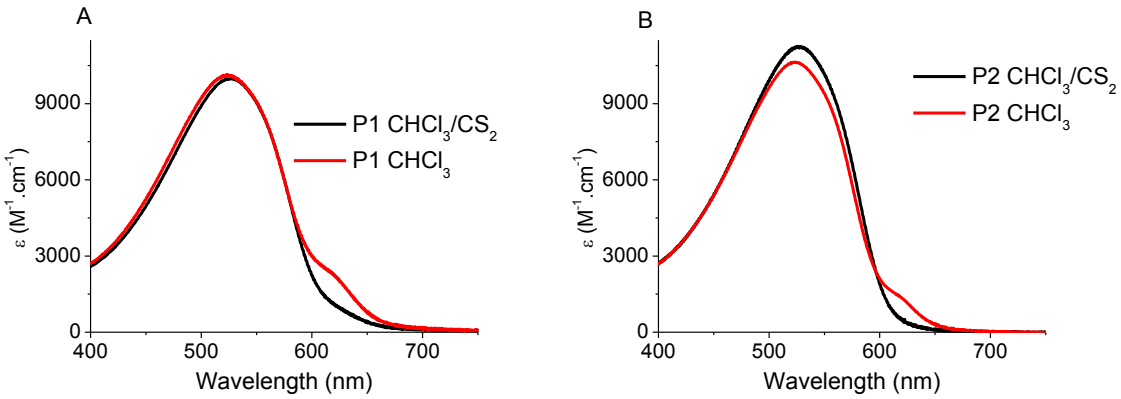

Figure S 9. Complete dissolution of **P1**(A) and **P2**(B) in $CHCl_3/CS_2$ vs **P1** in $CHCl_3$.

S4. Solvatochromism experiment of P1-5

S4.1 Solvatochromism

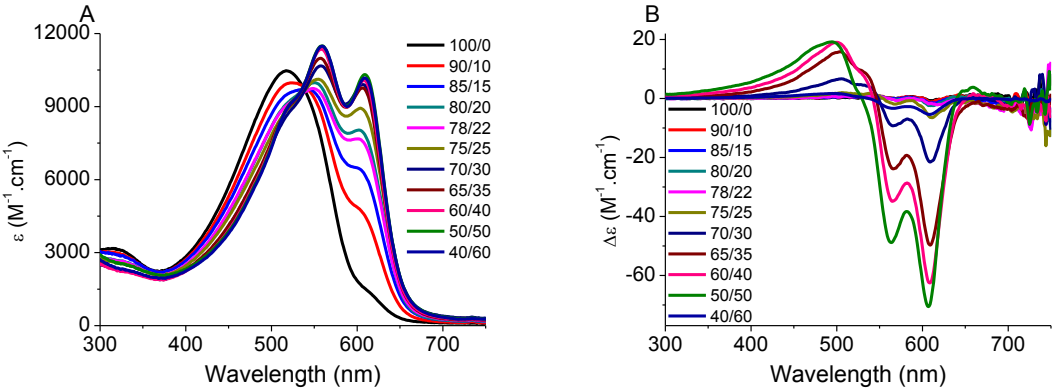

Figure S 10. Solvatochromism experiment of **P1** in $CHCl_3$/MeOH mixtures: A) UV-vis spectra and B) CD spectra.

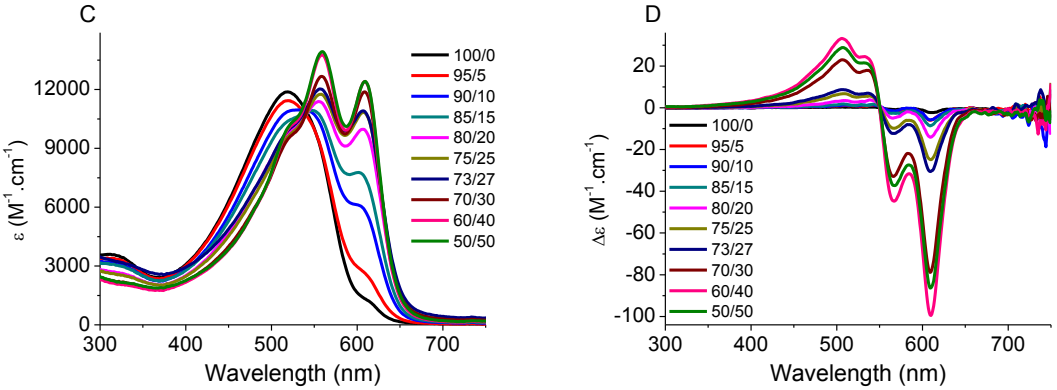

Figure S 11. Solvatochromism experiment of **P2** in $CHCl_3$/MeOH mixtures: C) UV-vis spectra and D) CD spectra.

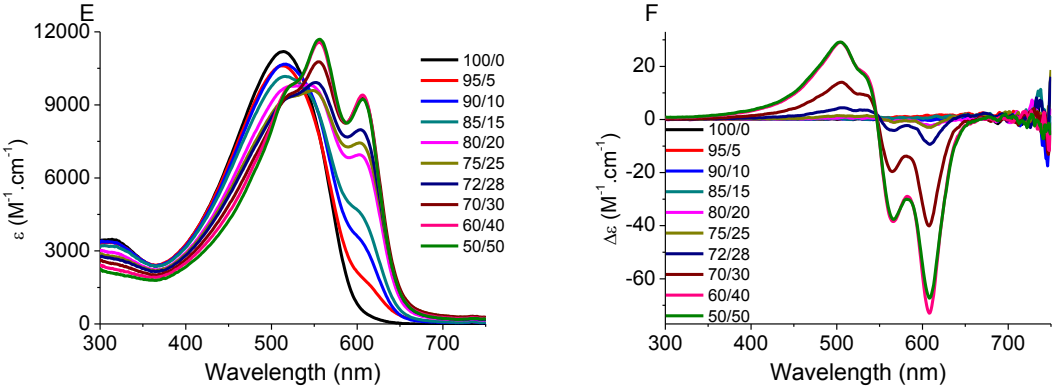

Figure S 12. Solvatochromism experiment of **P3** in $CHCl_3$/MeOH mixtures: E) UV-vis spectra and F) CD spectra.

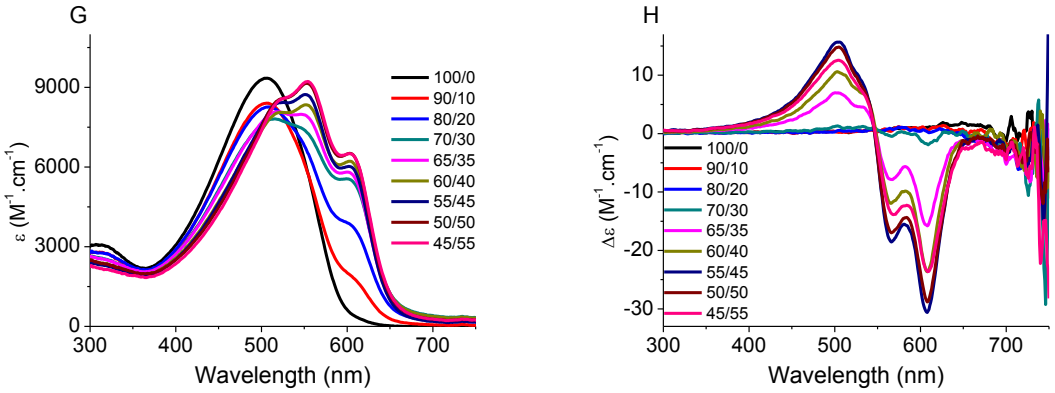

Figure S 13. Solvatochromism experiment of **P4** in $CHCl_3$/MeOH mixtures: G) UV-vis spectra and H) CD spectra.

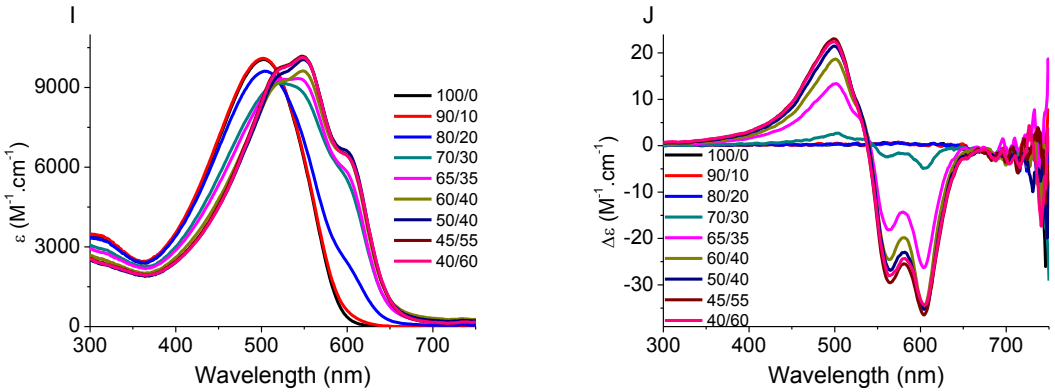

Figure S 14. Solvatochromism experiment of **P5** in $CHCl_3$/MeOH mixtures: I) UV-vis spectra and J) CD spectra.

S4.2 Deconvolution of UV-vis spectra of P1-P5

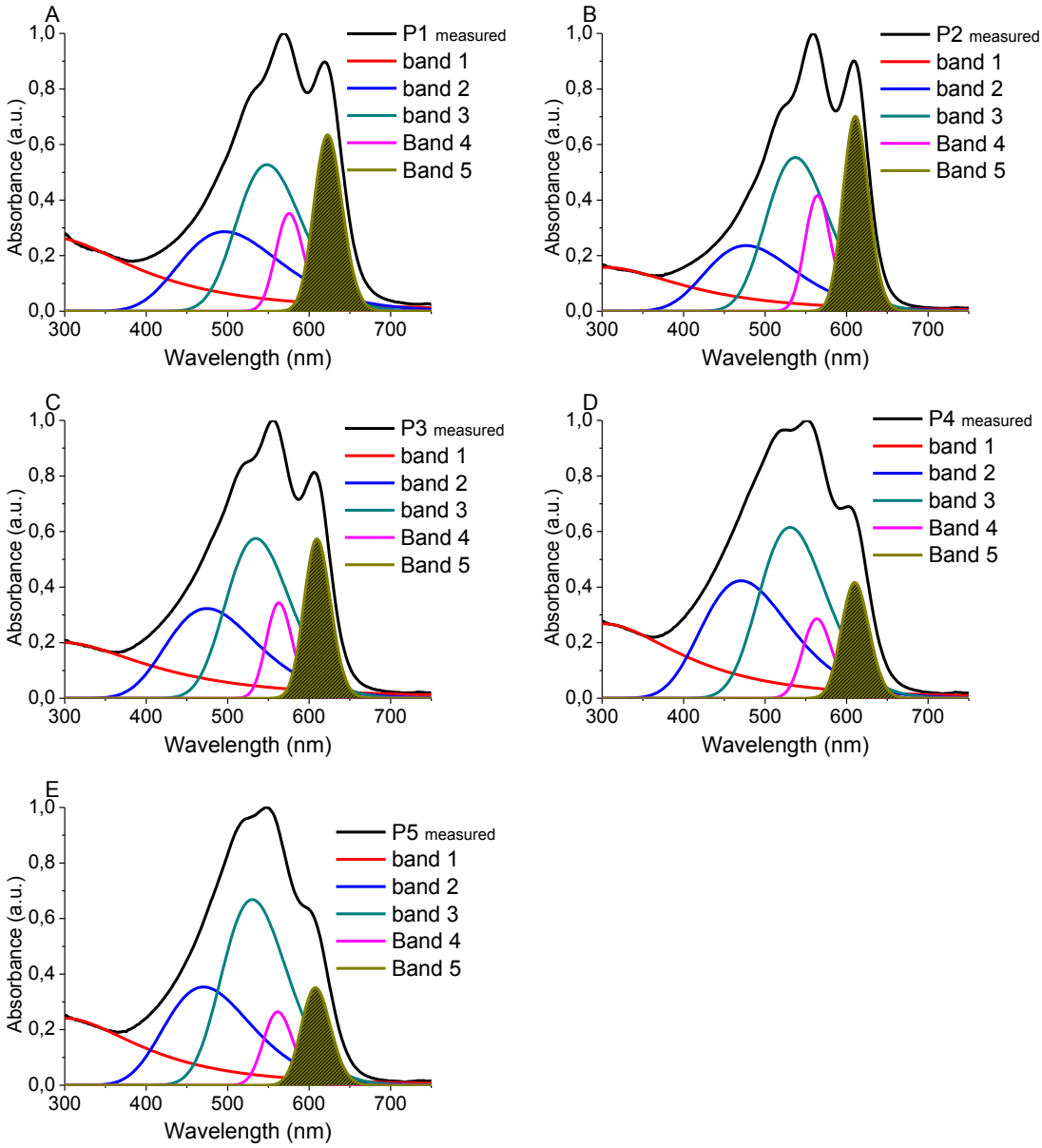

Figure S 15. Deconvolution of UV-vis spectra of P1-P5 in poor solvent mixtures. The band near 610 nm, which probes π interactions, was filled and the relative integration was calculated. A) **P1** $CHCl_3$/MeOH (50/50); 15.3%, B) **P2** $CHCl_3$/MeOH (60/40); 17.8%, C) **P3** $CHCl_3$/MeOH (60/40); 13.5%, D) **P4** $CHCl_3$/MeOH (55/45); 9.2%, E) **P5** $CHCl_3$/MeOH (45/55); 8.9%.

S5. Emission spectroscopy of P1-P5

S5.1 Emission spectroscopy of P1-P5 in $CHCl_3$

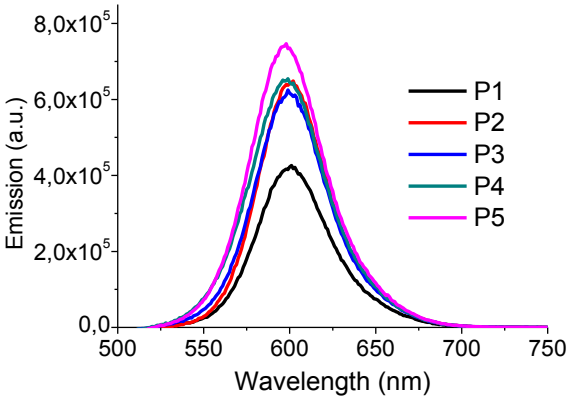

Figure S 16. Emission spectra of **P1-P5** in $CHCl_3$ excited at 500 nm.

S5.2 Emission spectroscopy of P1 in $CHCl_3/CS_2$ (8/2)

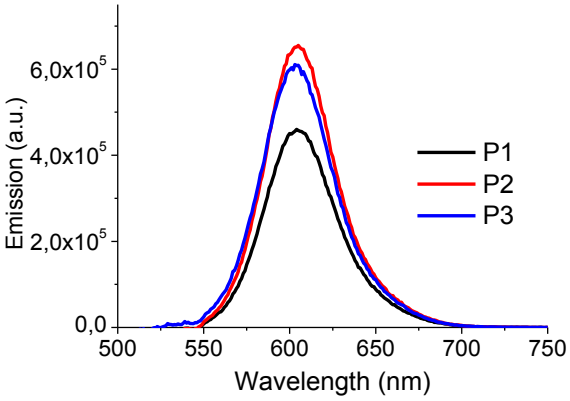

Figure S 17: Emission spectra of **P1-P3** in $CHCl_3/CS_2$ (8/2) excited at 500 nm.

S6. IR spectra of P1-P5

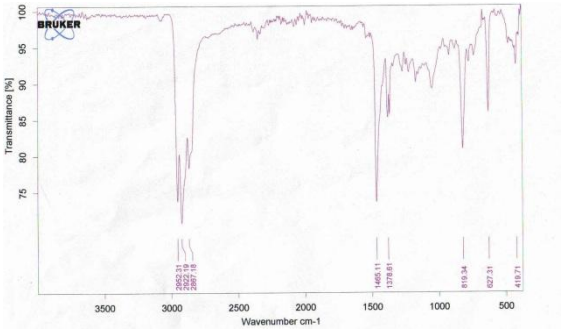

Figure S 18. IRspectrum P1.

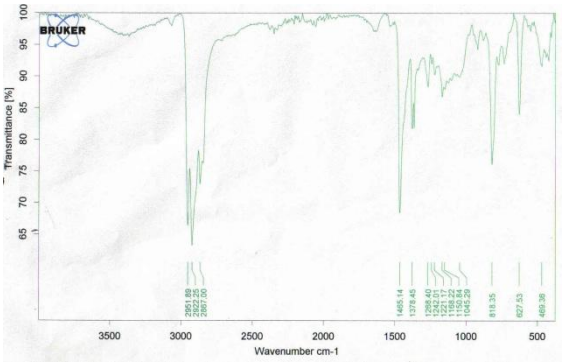

Figure S 22. IRspectrum P1.

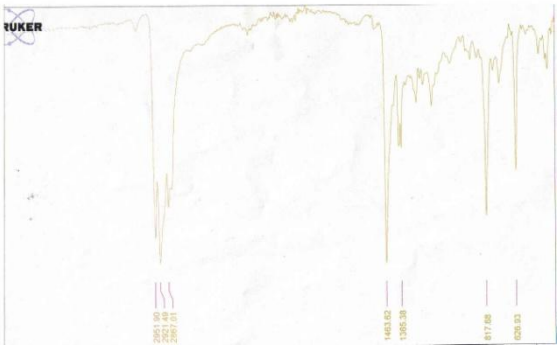

Figure S 19. IRspectrum P2.

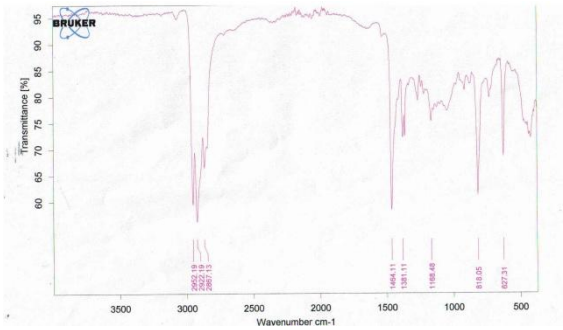

Figure S 20. IRspectrum P3.

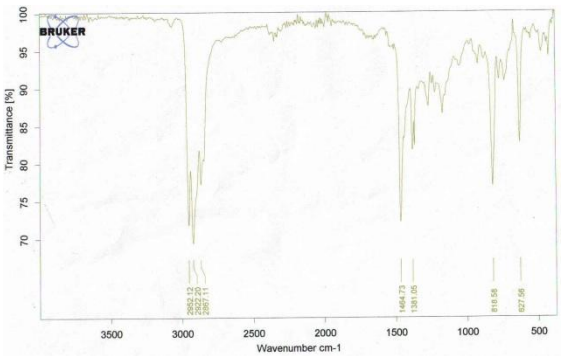

Figure S 21. IRspectrum P3.